Identification of Mass-Spring-Damper Model of Walking Humans

Erfan Shahabpoor[1], Aleksandar Pavic[2], Vitomir Racic[3]

[1]Research associate, INSIGNEO Institute for In-Silico Medicine, Department of Civil & Structural Engineering, University of Sheffield, UK
[2]Professor of Vibration Engineering, College of Engineering, Mathematics and Physical Sciences, University of Exeter, UK
[3]Associate Professor, Department of Civil and Environmental Engineering, Politecnico di Milano, Italy. Department of Civil & Structural Engineering, University of Sheffield, UK

Contact author: E. Shahabpoor
                     Department of Civil & Structural Engineering
                     University of Sheffield
                     Sir Frederick Mappin Building
                     Sheffield S1 3JD
                     E-mail: e.shahabpoor@sheffield.ac.uk
                     Tel: 0114-2225745
                     Fax: 0114-2225700

Body text word count:	5258
Number of figures:	16
Number of tables:	6

32   **Abstract**

33   Interaction of walking people with vibrating structures is known to be an important yet

34   challenging phenomenon to simulate. Despite of its considerable effects on the

35   structural response, no properly formulated and experimentally verified model currently

36   exists to simulate this interaction in the vertical direction.

37   This work uses a single-degree-of-freedom mass-spring-damper model of a walking

38   human to simulate its interaction with a vibrating structure. Extensive frequency

39   response function measurements were performed on a test structure that was occupied

40   by more than a hundred tests subjects walking in various group sizes and at different

41   times in 23 tests. The identified modal properties of the occupied structure were used in

42   three different identification procedures to estimate the parameters of the walking

43   human model.

44   A discrete model of human – structure system was used to simulate interaction of each

45   walking person with the structure. The analysis identified the range of 2.75 – 3.00 Hz

46   for the natural frequency and 27.5 % – 30% for the damping ratio of the model of a

47   walking human, having constant mass of 70kg. The extent of the experimental data and

48   the measurement details, diversity of loading scenarios and consistency of the results of

49   the different identification procedures, provided high level of confidence on the

50   suggested parameters for the single-degree-of-freedom walking human model.

1 Introduction

Vibration serviceability of structures under a range of different human activities has been a growing concern to civil structural engineers since 19th century [1, 2]. The current design trends towards more slender and longer span structures have made them more susceptible than ever before to vibration serviceability problems [3, 4, 5, 6]. Investigations of several recent incidences due to walking pedestrians, both in the vertical and lateral directions, have highlighted the inability of the contemporary design guidelines to estimate reliably the vibration response [7, 8]. The key reason for this unsatisfactory situation is a widespread, yet utterly wrong, assumption that walking people affect structural dynamics only through the inertia of their moving bodies, thereby acting only as the main source of the vibration [4]. In reality, the human bodies have equally powerful effect on the modal properties of the occupied structure which, as this paper will demonstrate, should not be ignored [8, 9, 10, 11].

The simplest walking load models, such as those suggested by FIB [12], ISO 10137 [13], French design guideline [14] and UK National Annex to Eurocode 1 [15], approximate the walking force of an individual with a periodic function presentable via up to four dominant Fourier harmonics. Typically, one of these harmonics is tuned to match the frequency of a target mode of the structure to create resonance. In case of a multi-pedestrian traffic, the net force is most commonly calculated by multiplying the individual walking force by factor(s) which often depend on the pedestrian density on the structure [4, 16].

A significant move towards more realistic estimation of the structural response was made only recently by taking into account inter- and intra- subject variability of the pedestrians in the form of statistical models of their walking force [6, 17, 18, 19, 20, 21, 22]. This has increased considerably the fidelity of the walking force models, but they still cannot account fully for the human-structure interaction (HSI) [8, 11].

79   Mass of a stationary human body accelerates when exposed to vertical structural

80   vibration, thereby creating an interaction force at the contact point with the structure

81   [23]. The same applies to the moving people, in which case additional ground reaction

82   force is created due to the self-propelling body motion. These interaction forces

83   manifest as changes in the modal frequency of the empty structure (i.e. through the

84   alteration of modal mass and/or stiffness) and damping. This is because such forces

85   have components proportional to acceleration, velocity and displacement as well as

86   independent components [24]. There have been several successful studies designed to

87   quantify changes of the modal properties of structures when occupied by stationary (e.g.

88   standing or sitting) people [25, 26, 27, 28, 29]. The results consistently suggested a more

89   or less significant increase in structural damping and shifting of the natural frequency

90   in, surprisingly, either direction. Experimental and analytical studies prompted by the

91   Millennium Bridge problem [30] reported that walking people also add considerable

92   damping when they excite lateral vibration modes of a structure [31]. However, similar

93   studies on the effect of walking people on the vertical structural modes are very rare and

94   limited [32, 33].

95   Zivanovic, et al. [33] did a series of FRF measurements on a test footbridge and studied

96   the changes in the dynamic properties of the structure in the vertical direction due to the

97   presence of either *all* standing or *all* walking groups of people. They reported a slight

98   increase in the natural frequency and a three-fold increase of the damping of the

99   occupied structure relative to the empty structure. Moreover, the authors observed that

100   the walking people added less damping to the structure than the stationary people. Based

101   on an analytical study featuring a walking human as a single-degree-of-freedom (SDOF)

102   mass-spring-damper (MSD) oscillator, Shahabpoor, et al. [34, 35] showed that the

103   natural frequency of a vertical mode of the occupied structure can either increase or

104   decrease depending on the frequency of the human SDOF system, while damping of the

4

105 structure always increases. These changes appeared prominent especially when the

106 natural frequency of the human SDOF system was close to the modal frequency of the

107 empty structure.

108 Miyamori, et al. [36] reported similar results using a more complex 3DOF biodynamic

109 model of a walking individual, but also without experimental verification. Kim, et al.

110 [37] used a simpler 2DOF MSD model with little success because the majority of the

111 human model parameters were adapted from ISO 5982:1981 [38], which refers to

112 stationary standing (rather than walking) people. Favored for its simplicity, the

113 elementary SDOF MSD model was used in a number of studies to simulate pedestrian-

114 structure interaction in the vertical direction [17, 39, 40, 41, 42, 43, 44]. However, due

115 to the lack of knowledge about the true values of the parameters of a walking human

116 SDOF system, the values were either assumed or adapted from sparse biomechanical

117 studies relevant to other activities, such as bouncing and jumping. The work of Silva

118 and Pimentel [41] and Jiménez-Alonso and Sáez [44] are the only examples to date

119 known to the authors that proposed a range of parameters for the SDOF walking human

120 model in the context of structural vibration serviceability. However, the suggested

121 values were derived using the inadequate analogy with stationary people and are based

122 on several weak assumptions, such as that the walking excitation is a single sine wave.

123 All of these studies commonly lack verification against a sufficiently large and

124 statistically reliable experimental walking data recorded in parallel with structural

125 vibration response.

126 In recent years there have been several attempts to use biomechanical models such as

127 the inverted pendulum (IP) model that swings in the vertical plane [45, 46, 47, 48].

128 Apart from the lack of adequate experimental validation, non-linear interaction

129 mechanism which is an essential part of these models is not straightforward for

130 implementation in design practice. Moreover, the credibility of results of IP models is

131 usually compromised by the large number of assumptions necessary for their simulation

132 such as the regulatory control force to maintain the steady walking gait and initial energy

133 input.

134 Moving from the single walking person to multi-pedestrian walking traffic, real

135 stochastic nature of relevant modelling parameters need to be considered. Variability of

136 the human mass m_h, damping c_h and stiffness k_h between different people and even for

137 the same person under different walking scenarios, interaction of people with each other

138 and time-varying location of people on the structure, all make the human traffic-

139 structure system highly complex. Challenges of modelling such essentially non-

140 deterministic system have forced design guidelines to use simplistic assumptions to

141 approximate the reality. Most of the load models, such as ISO [13], aggregate the effects

142 of pedestrians in a walking traffic and model their net sum loading as a single force. UK

143 National Annex to Eurocode 1 [15] and FIB [12] go further and specify "scaling factors"

144 of the force magnitude to account for possible synchronization between pedestrians.

145 The works by Paulissen and Metrikine [49] and Pecol et al. [50], pertinent to the lateral

146 direction, and by Caprani et al. [43], Silva, et al. [42] and Jiménez-Alonso and Sáez

147 [44] pertinent to the vertical direction are very rare recent attempts to model discrete

148 walking traffic load by simulating every individual.

149 In conclusion, no fully developed, well elaborated and experimentally verified model

150 exists currently to simulate reliably enough the effects of the walking human in the

151 *vertical* direction for a diverse range of loading scenarios and structures. This is mainly

152 due to the challenging nature of collecting experimental data pertinent to walking people

153 – the issue that the present study specifically aims to address.

154 This paper uses comprehensive measurements of pedestrian flow recorded on a

155 laboratory-based, yet realistic, 15-tonne prototype footbridge structure. The location on

156   the structure and speed of each pedestrian at every moment of time, their weight and the

157   corresponding 'nominally identical' walking force on a stiff surface were recorded for

158   all tests. Moreover, acceleration response of the structure was recorded in parallel to the

159   walking data. A discrete traffic model was used to simulate walking people in which

160   each individual is modeled as a SDOF MSD oscillator. By fitting the analytical

161   Frequency Response Function (FRF) of the occupied structure to its experimental

162   counterparts, the unknown natural frequency f_h and damping ratio ζ_h of the SDOF

163   human oscillator were identified using three optimization methods.

164   Section 2 of this paper presents a brief description of two experimental campaigns and

165   the selection of results used in this paper. In Section 3.1 the proposed identification

166   procedures and the discrete walking traffic-structure model are described in detail.

167   Results of the analysis are presented for two 'stationary' and 'moving' walking

168   scenarios in Sections 3.2 and 3.3, respectively, while values of the identified parameters

169   for each human SDOF model are determined and discussed in Section 3.4. Finally, the

170   conclusions are presented in Section 5.

171   2   Experimental campaigns

172   Two series of tests (referred to as Series 'A' and 'B'), separated by approximately a

173   year, were carried out on the Sheffield University prototype test footbridge (Figure 1)

174   at different times but with identical test setup. Each series comprised a set of FRF-based

175   modal tests of the empty structure and the structure when a number of people were

176   walking on it. In total 23 tests were carried out: 13 tests focused on the first mode and

177   10 tests focused on the second mode. In these tests between 2 and 15 people were

178   walking on the structure and modal properties of the occupied structure were estimated

179   experimentally.

180
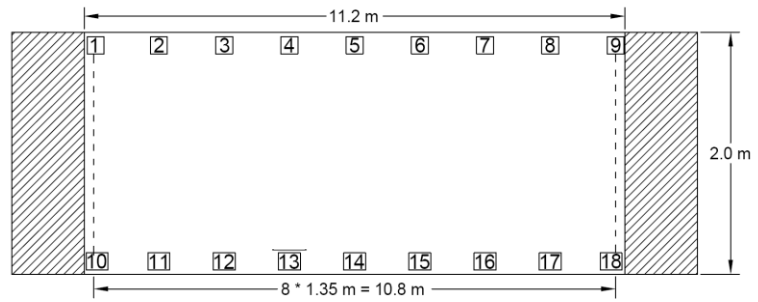
Figure 1: Photo, plan and modal test grid of the Sheffield footbridge. Two side platforms are shown with hatched rectangles.

181

2.1   Empty structure

183   The structure used in this study is a simply supported in-situ cast post-tensioned

184   concrete footbridge purposely built in the structures laboratory of the University of

185   Sheffield. The structure rests on two knife edge supports along its shorter edges, as

186   illustrated in Figure 1 and behaves like a simply supported beam. The total length of the

187   footbridge is 11.2m, including short 200 mm overhangs at the supports. Its rectangular

188   cross section has width of 2.0 m and depth of 275 mm, and it weighs approximately 15

189   tonnes.

190   Previous modal tests of the Sheffield footbridge [11] showed that it has four modes of

191   vibration (Figure 2) with modal frequencies less than 50 Hz. Only the first two vertical

192   modes with modal frequencies 4.44 Hz and 16.8 Hz were considered relevant for this

193   study. In each test series, a set of FRF-based modal testing was conducted on the empty

194   footbridge using 18 Honeywell QA 750 accelerometers placed parallel to the longer

195   edges of the slab (Figure 1).

196

197

a) First vertical mode shape @ 4.44 Hz

b) Second vertical mode shape @ 16.8 Hz

c) First torsional mode shape @ 25.9 Hz
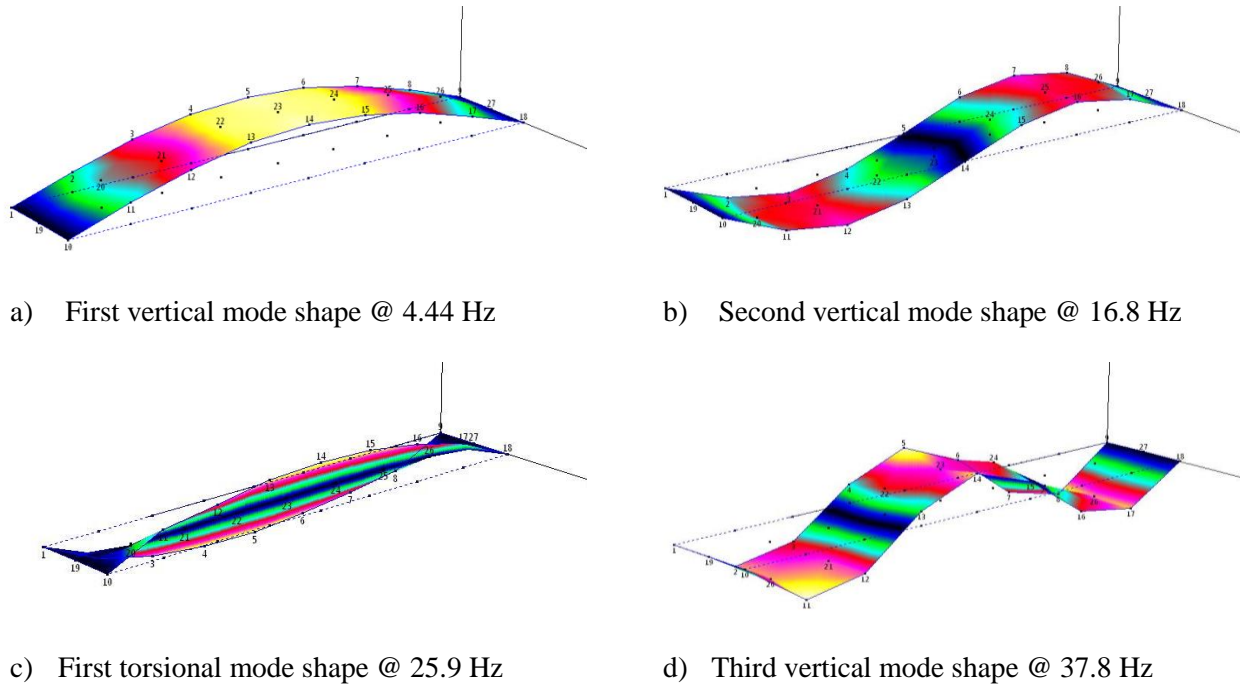
d) Third vertical mode shape @ 37.8 Hz

Figure 2: Experimentally acquired mode shapes of PT slab

198 In each test series A and B, two FRF-based modal tests were carried out, one for the

199 first and one for the second mode. Chirp signals with the frequency ranges of 3.5 –

200 5.5 Hz for the first vertical mode (4.44 Hz), and 15 – 18 Hz range for the second vertical

201 mode (16.8 Hz) were used to excite the structure. An APS electro-dynamic shaker

202 model 400 [51], operated in the direct-drive mode, was connected to the slab from

203 beneath at the mid-span or the quarter-span to get the highest possible excitation at the

204 anti-node of the mode 1 or mode 2, respectively. The point mobility FRF was used to

205 estimate modal properties. Empty structure modal properties are presented in Table 1

206 for both Series A and B tests. A slight difference between the identified modal properties

207 of the empty structure is noticeable between Series A and B which is to be expected

208 considering the time gap of about a year between the tests.

209

Table 1: Results of modal analysis of the empty structure (es)

Mode	FRF based						
#	Modal frequency f_{es}(Hz)	Modal damping ratio ζ_{es} (%)	Modal mass m_{es} (kg)	Modal damping coefficient c_{es} (N.s/m)	Modal stiffness k_{es} (N/m)	Maximum response a_{max} (m/s^2)	Response RMS a_{rms} (m/s^2)
1 (Series A)	4.44	0.6	7,128	2,386	5,547$\times 10^3$	1.8782	0.3680
1 (Series B)	4.44	0.7	7,128	2,784	5,547$\times 10^3$	2.6084	0.4826
2 (Series A)	16.87	0.4	7,128	6,044	80,086$\times 10^3$	2.5080	0.4769
2 (Series B)	16.77	0.4	7,128	6,009	79,140$\times 10^3$	3.2123	0.5942

210

2.2   Pedestrian data

The weight of each pedestrian was measured using a simple digital weighing scale. The

walking force of each person (for their self-selected 'comfortable' walking speed) on a

stiff surface was recorded using an instrumented treadmill. A pair of PeCo laser

pedestrian counters [52], located 8 meters apart above the footbridge walkway (Figure

3), were used to record the time- and direction-stamped instances of each pedestrian
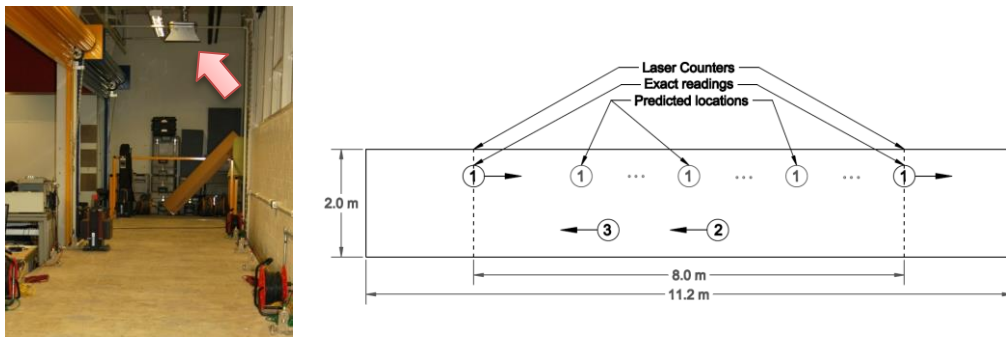
crossing them.

Figure 3: Prediction of people location between each two consecutive crossing of
PeCo laser pedestrian counter

218

Figure 4 presents typical time-histories of location of three pedestrians during a 100s

test. Location of each person is shown with different colour and support locations are

shown with dashed lines. Time-history of each pedestrian location and walking speed

were calculated by cross-comparing the PeCo data with the synchronized time-stamped

223 video footage of each test. Walking speed was assumed constant between each two

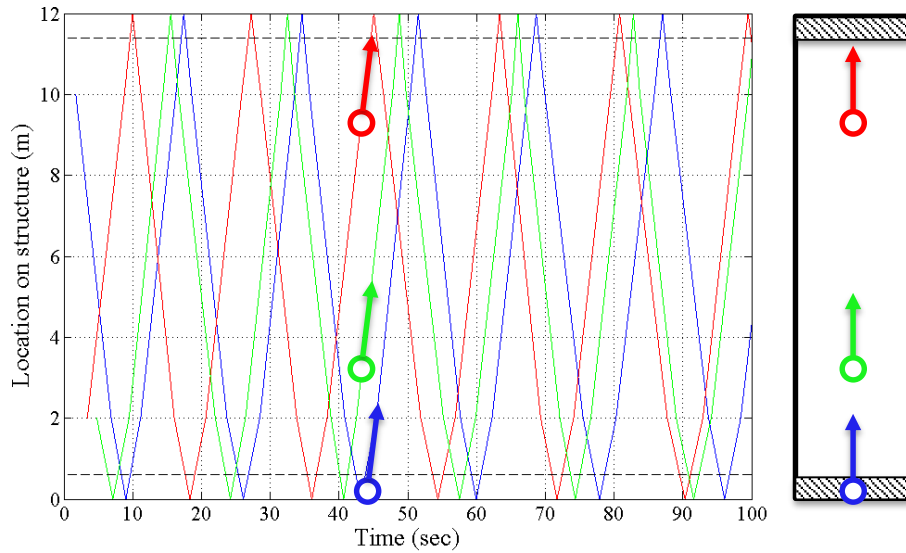224 consecutive crossings of the laser counters.

Figure 4: A typical time-history of location of three pedestrians on the structure
presented with three different colors

225

2.3   Occupied structure tests

227 Two different loading scenarios were considered for this study. In the first loading

228 scenario test participants were asked to walk around a tight circle in specific locations

229 on the structure (mid-span, quarter-span and 3/8 span). In this loading scenario, people

230 were assumed to be *nominally stationary* on the structure i.e. their locations on the

231 structure were constant and assumed to be at the center of the circle (Figure 5a). This

232 assumption is important as it eliminates the time-variance in the model of the human-

233 structure system and makes it possible to formulate their dynamic interaction using

234 conventional equation of motions for linear multiple-degrees-of-freedom (MDOF)

235 systems. Eight tests, five focused on the first mode of the structure and three focused on

236 the second mode, were carried out using this loading scenario. These tests were labeled

237 with letter 'C' at the end of their test number to indicate walking in a circle (Table 2).

238   In the second loading scenario test participants were asked to walk in a closed-loop path

239   along the structure (Figure 5b). Eight out of 15 tests targeted the first vertical vibration

240   mode, while the remaining seven tests focused on the second vertical mode of vibration.

241   Between 2 and 15 people participated in each test. They were asked to walk with their

242   comfortable speed and were free to pass each other. 15 data blocks, each lasting 64

243   seconds, were acquired in each test to average out unmeasured extraneous excitation as

244   much as possible and get better quality FRFs. The FRF test setups were identical to the

245   empty structure tests with 18 accelerometers recording responses along the two long

246   edges of the structure (Figure 5).
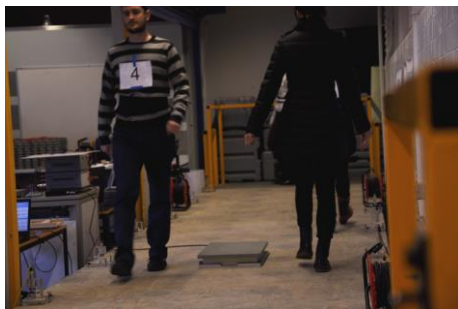
a)   Scenario 1: Walking in tight circle
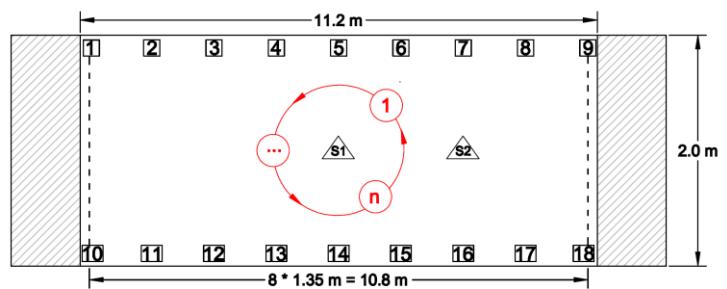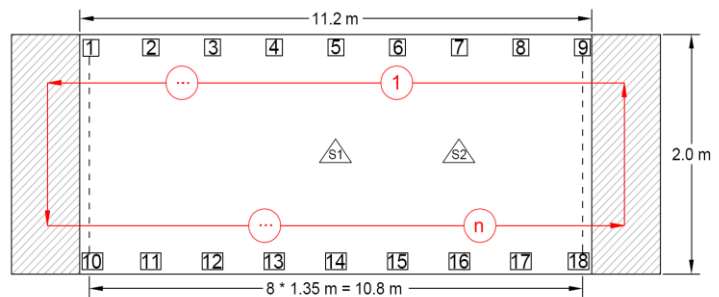

b)   Scenario 2: Walking along the structure

Figure 5: A typical walking path of designed loading scenarios

247

248

12

Table 2: Modal properties of the occupied structure (os) for different group sizes – walking around the tight circle tests

Test No.	Series	Location	No. of Pedestrians	Modal properties of the occupied structure (os)					Structural Response	
				f_{os} (Hz)	ζ_{os} (%)	m_{os} (kg)	c_{os} (N.s/m)	k_{os} (N/m)	a_{max} (m/s^2)	a_{rms} (m/s^2)
Mode 1 (Structure)										
1.1C	B	Mid-span	3	4.455	2.00	7,214	8,077	$5,652 \times 10^3$	1.3226	0.2488
1.2C	B	Mid-span	6	4.480	2.90	7,300	11,918	$5,784 \times 10^3$	1.0903	0.2008
1.3C	B	Mid-span	10	4.500	3.40	7,415	14,256	$5,928 \times 10^3$	0.8656	0.1861
1.4C	B	3/8 -span	6	4.465	2.50	7,287	10,222	$5,735 \times 10^3$	0.9920	0.1987
1.5C	B	Quarter-span	6	4.460	2.05	7,250	83,29	$5,693 \times 10^3$	1.0996	0.2195
Mode 2 (Structure)										
2.1C	B	Quarter-span	3	16.913	0.61	7,128	9,241	$80,496 \times 10^3$	2.2306	0.4188
2.2C	B	Quarter-span	6	16.925	0.82	7,128	12,432	$80,611 \times 10^3$	1.9406	0.3544
2.3C	B	Quarter-span	10	16.975	0.99	7,128	15,054	$81,091 \times 10^3$	1.6871	0.3660

249

250 Modal parameters of the occupied structure (OS), natural frequency f_{os} [Hz], modal mass

251 m_{os} [kg] and modal damping ratio ζ_{os} [%], were found by curve-fitting the point-mobility

252 FRF for each test. These parameters are presented in Table 2 and Table 3 for the tight-

253 circle (Figure 5a) and along the structure (Figure 5b) scenarios, respectively. Comparing

254 the values of modal properties of the occupied (Table 2 and Table 3) and empty structure

255 (Table 1), differences in the corresponding modal frequencies and particularly in

256 damping ratios are noticeable. These changes were attributed to the effects of the HSI

257 during walking. The identification methods developed for this paper (described in

258 Section 0) have used these observed effects to estimate the possible properties of the

259 human SDOF MSD model.

260

261

262

263

264

Table 3: Modal properties of the occupied structure (os) for different group sizes – 'walking along the structure' tests

Test No.	Series	Location	No. of Pedestrians	Modal properties of the occupied structure (os)					Structural Response	
				f_{os} (Hz)	ζ_{os} (%)	m_{os} (kg)	c_{os} (N.s/m)	k_{os} (N/m)	a_{max} (m/s^2)	a_{rms} (m/s^2)
Mode 1 (Structure)										
1.1	A	All-over	2	4.443	1.00	7,165	4,000	$5,583 \times 10^3$	2.4361	0.4131
1.2	B	All-over	3	4.445	1.10	7,183	4,413	$5,603 \times 10^3$	1.7489	0.3018
1.3	A	All-over	4	4.450	1.28	7,201	5,154	$5,630 \times 10^3$	2.1755	0.3637
1.4	A	All-over	6	4.465	1.55	7,238	6,294	$5,696 \times 10^3$	1.8771	0.3311
1.5	B	All-over	6	4.465	1.65	7,238	6,701	$5,696 \times 10^3$	1.4882	0.2481
1.6	B	All-over	10	4.475	2.30	7,311	9,456	$5,780 \times 10^3$	1.1313	0.2050
1.7	A	All-over	10	4.476	2.10	7,311	8,635	$5,782 \times 10^3$	1.5876	0.2870
1.8	A	All-over	15	4.485	2.91	7,402	12,140	$5,878 \times 10^3$	1.1251	0.2466
Mode 2 (Structure)										
2.1	B	All-over	3	16.900	0.55	7,128	8,326	$80,372 \times 10^3$	2.4059	0.4482
2.2	A	All-over	6	16.813	0.53	7,128	7,982	$79,548 \times 10^3$	2.9046	0.5595
2.3	B	All-over	6	16.910	0.65	7,128	9,846	$80,468 \times 10^3$	2.2905	0.4234
2.4	A	All-over	8	16.819	0.61	7,128	9,190	$79,605 \times 10^3$	2.5591	0.5133
2.5	A	All-over	10	16.822	0.64	7,128	9,644	$79,634 \times 10^3$	2.5232	0.5223
2.6	B	All-over	10	16.935	0.75	7,128	11,377	$80,708 \times 10^3$	2.1387	0.4023
2.7	A	All-over	15	16.825	0.79	7,128	11,907	$79,665 \times 10^3$	2.2358	0.4725

266

2.4 Changes of mode shapes

One of the key assumptions of the identification methods used in this paper was that the presence of walking people on a structure did not affect its mode shapes. This assumption was examined by comparing the mode shapes of the empty structure and when occupied by a group of 10 (Figure 6). The acceleration responses recorded by all 18 accelerometers on the structure were used to find the first two mode shapes. The mode shape amplitudes were calculated at nine equidistant points along the central longitudinal axis of the symmetry of the footbridge. They were average values of the two mode shapes each measured at nine points along the two edges of the footbridge (eg. 10 and 1, 11 and 2, etc.). As it can be seen in Figure 6, there is no significant difference between the mode shapes of the empty and the occupied structure.

Moreover, another assumption was made that, for a given number of people walking across the structure, the modal properties of the occupied structure m_{os} [kg], c_{os} [Ns/m]

280   and k_{os} [N/m], determined from measured FRFs, represent their *average* over the test

281   duration. This assumption holds despite the fact that people's location change
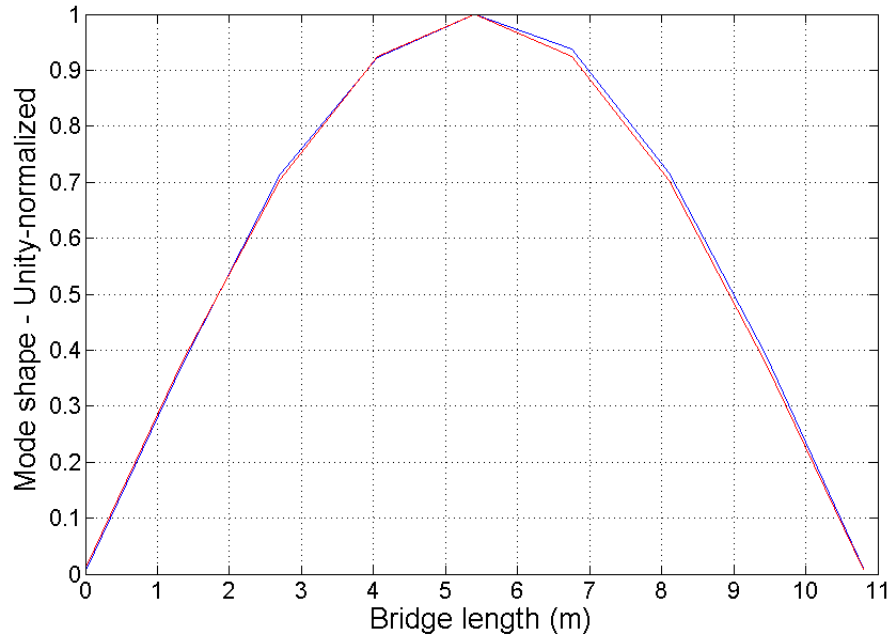
282   continuously with time.

Figure 6: First mode shape of empty (blue trace) and occupied (red trace) Sheffield footbridge

283

3   Identification of walking human model

285   The core of all the identification procedures developed for this study is a 'stationary'

286   walking traffic-structure model. It describes an abstract situation in which people walk

287   on a spot, i.e. their location on the structure does not change. It can be imagined as

288   people walking on a series of treadmills installed at fixed locations on a structure (Figure
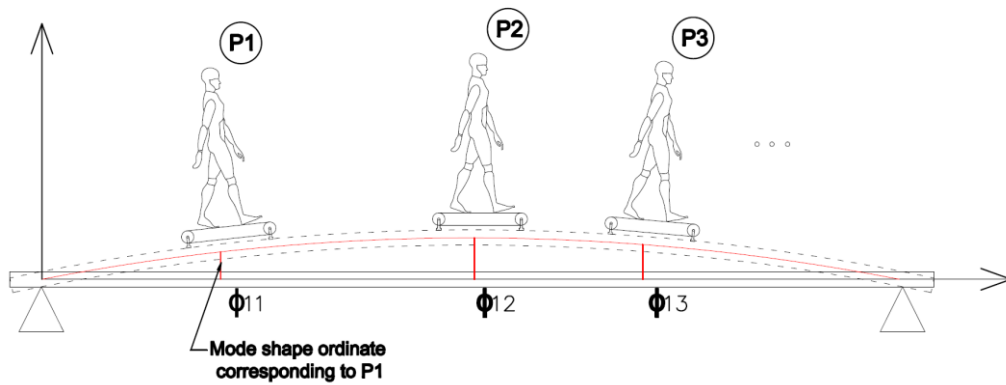
289   7).

15

Figure 7: A conceptual illustration of stationary walking people

290

291   Figure 8 presents the MSD model of such a stationary walking traffic-structure system.

292   The SDOF MSD model was used to simulate dynamics of each walking individual on

293   the structure. Similarly, an SDOF model was used to simulate one mode of the structure

294   at a time. The effects of the location of each individual on the structure were taken into

295   account by scaling their parameters (m_h, c_h and k_h) and excitation amplitudes with the

296   ordinate of the mode shape corresponding to their location on the structure (Φ in Figure

297   7 and), as appropriate in modal analysis.
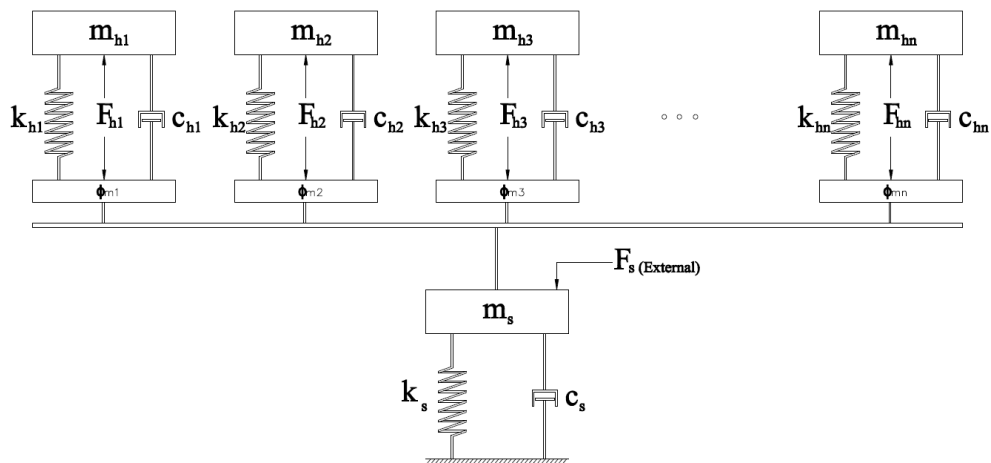

Figure 8: MDOF Mass-spring-damper model of stationary walking traffic-structure system

298

299   Being stationary, this system could be treated as a conventional MDOF system

300   (Equation 1). A modified system of equations of motion (Equation 2) was developed

301   that takes into account the location of people on the structure:

302     $[M]\{\ddot{x}(t)\} + [C]\{\dot{x}(t)\} + [K]\{x(t)\} = \{F(t)\}$ (Eq. 1)

303
$$\begin{bmatrix} m_{es,j} & 0 & 0 & \cdots & 0 \\ 0 & m_{h1} & 0 & \cdots & 0 \\ 0 & 0 & m_{h2} & \cdots & 0 \\ \vdots & \vdots & \vdots & \ddots & \vdots \\ 0 & 0 & 0 & \cdots & m_{hn} \end{bmatrix} \begin{bmatrix} \ddot{x}_{os,j}(t) \\ \ddot{x}_{h1}(t) \\ \ddot{x}_{h2}(t) \\ \vdots \\ \ddot{x}_{hn}(t) \end{bmatrix} +$$

304
$$\begin{bmatrix} c_{es,j} + (c_{h1} \times \varphi_{1j}) + (c_{h2} \times \varphi_{2j}) + \cdots + (c_{hn} \times \varphi_{nj}) & -(c_{h1} \times \varphi_{1j}) & -(c_{h2} \times \varphi_{2j}) & \cdots & -(c_{hn} \times \varphi_{nj}) \\ -(c_{h1} \times \varphi_{1j}) & c_{h1} & 0 & \cdots & 0 \\ -(c_{h2} \times \varphi_{2j}) & 0 & c_{h2} & \cdots & 0 \\ \vdots & \vdots & \vdots & \ddots & \vdots \\ -(c_{hn} \times \varphi_{nj}) & 0 & 0 & \cdots & c_{hn} \end{bmatrix} \begin{bmatrix} \dot{x}_{os,j}(t) \\ \dot{x}_{h1}(t) \\ \dot{x}_{h2}(t) \\ \vdots \\ \dot{x}_{hn}(t) \end{bmatrix} +$$

305

306
$$\begin{bmatrix} k_{es,j} + (k_{h1} \times \varphi_{1j}) + (k_{h2} \times \varphi_{2j}) + \cdots + (k_{hn} \times \varphi_{nj}) & -(k_{h1} \times \varphi_{1j}) & -(k_{h2} \times \varphi_{2j}) & \cdots & -(k_{hn} \times \varphi_{nj}) \\ -(k_{h1} \times \varphi_{1j}) & k_{h1} & 0 & \cdots & 0 \\ -(k_{h2} \times \varphi_{2j}) & 0 & k_{h2} & \cdots & 0 \\ \vdots & \vdots & \vdots & \ddots & \vdots \\ -(k_{hn} \times \varphi_{nj}) & 0 & 0 & \cdots & k_{hn} \end{bmatrix} \begin{bmatrix} x_{os,j}(t) \\ x_{h1}(t) \\ x_{h2}(t) \\ \vdots \\ x_{hn}(t) \end{bmatrix} =$$

307
$$\begin{bmatrix} f_{ex,j}(t) + (f_{h1}(t) \times \varphi_{1j}) + (f_{h2}(t) \times \varphi_{2j}) + \cdots + (f_{hn}(t) \times \varphi_{nj}) \\ 0 \\ 0 \\ \vdots \\ 0 \end{bmatrix}$$ (Eq. 2)

308   In Equation 2, $m_{es,j}$, $c_{es,j}$ and $k_{es,j}$ are mode j modal mass, damping coefficient and

309   stiffness of the empty structure (es) and m_{hi} , c_{hi} and k_{hi} are those of the walking

310   individuals. Viscous damping is assumed for SDOF walking human models. $\ddot{x}_{os,j}(t)$,

311     $\dot{x}_{os,j}(t)$ and $x_{os,j}(t)$ are the acceleration, velocity and displacement response of occupied

312   structure DOF in the system. As one mode of the structure (j) is simulated at a

313   time, $\ddot{x}_{os,j}(t)$, $\dot{x}_{os,j}(t)$ and $x_{os,j}(t)$ also represent the *modal response* of the occupied

314   structure. Similarly, $\ddot{x}_{hi}(t)$, $\dot{x}_{hi}(t)$ and $x_{hi}(t)$ represent acceleration, velocity and

315   displacement of the ith walking person DOF. $f_{ex,j}(t)$ is the mode 'j' modal force (if any)

316   due to an external force acting on the structural DOF and $f_{hi}(t)$ is a walking force of

317   person 'i' on a stiff surface. φ_{ij} is the ordinate of 'jth' mode shape of the structure at the

318   location of person 'i'.

319   The damping matrix of the system described by Equation 2 is not necessarily

320   proportional. Therefore, the conventional formulation of the proportionally-damped

321   eigenvalue problem will not yield modal vectors (eigenvectors) that uncouple the

322   equations of motion of the system [53]. The state-space technique used here to

323   circumvent this problem involves the reformulation of the original equations of motion,

324   for an N-degree of freedom system, into an equivalent set of 2N first order differential

325   equations [54].

326   In the first step, a new coordinate vector $\{y\}$ containing displacement $x(t)$ and velocity

327   $\dot{x}(t)$ is defined:

$$\{y(t)\} = \begin{Bmatrix} x(t) \\ \dot{x}(t) \end{Bmatrix} \qquad \text{(Eq. 3)}$$

328

329   Then Equation 2 is re-written into following form for modal analysis [54]:

$$\begin{bmatrix} [C] & [M] \\ [M] & [0] \end{bmatrix} \{\dot{y}(t)\} + \begin{bmatrix} [K] & [0] \\ [0] & [-M] \end{bmatrix} \{y(t)\} = \{0\} \qquad \text{(Eq. 4)}$$

330

331   In Equation 4, [M], [C] and [K] are the mass, damping and stiffness matrices of the

332   walking traffic-structure system, respectively, as detailed in Equation 2. Equation 4

333   leads to a standard eigenvalue problem and can be solved for eigenvectors and

334   eigenvalues accordingly. Further discussion of modal analysis of systems with non-

335   proportional damping is beyond the scope of this paper.

336   The MDOF system in has n+1 modes of vibration. The *dominant mode* of vibration

337   was defined as the mode with maximum response at the 'structure' degree of freedom.

338   For consistency and to allow for mode superposition, mode shapes were scaled in a way

339   that the ordinate of the structure DOF is 1.0. Such scaling ensured that modal properties

340   of the human-structure system are found with the same scaling as the empty structure.

3.1 Identification procedure

The identification procedure developed for this study was iterative by trial and error. Initial ranges of 1-10 Hz with 0.05 Hz steps for f_h and 5 - 70% with 2.5% steps for ζ_h were selected to model the walking human ('h' subscript is used here instead of 'hi' to refer generally to any human). These ranges were selected based on the values suggested in the biomechanics literature [36, 55, 56] and the study done by Silva, et al. [41] on walking people.

The MDOF traffic-structure model shown in was used to simulate each test and to estimate occupied structure parameters f_{os}, m_{os} and ζ_{os}. These parameters and peak FRF magnitude a_{FRF} were compared with their experimental counterparts and the corresponding errors were calculated. This process was repeated for all combinations of f_h and ζ_h for each test. The same values of f_h and ζ_h were used in each simulation for all pedestrians to reduce the number of combinations needing analysis and to make the results simpler to interpret. Mass of the human model m_h was assumed equal to the average mass of participants in the corresponding test. The values of the empty structure modal properties presented in Table 1 were used as m_{es}, k_{es} and c_{es}.

A series of maximum acceptable errors were defined for the estimated f_{os}, m_{os}, ζ_{os} and a_{FRF}. These were 0.01 Hz for f_{os}, 250 kg for m_{os}, 1% for ζ_{os} and 20% for a_{FRF}. For each test, the *ranges* of f_h and ζ_h were identified that predict f_{os}, m_{os}, ζ_{os} and a_{FRF} with errors less than the maximum acceptable. These ranges are referred to as 'test-accepted' ranges. In the next step, the test-accepted ranges of f_h and ζ_h were combined for all tests (each mode separately) and common ranges of f_h and ζ_h across all tests were found. This ensures that, if any combination of f_h and ζ_h (selected from these common ranges) was used to simulate people in any of the tests, the predicted f_{os}, m_{os}, ζ_{os} and a_{FRF} would be within the acceptable error ranges.

366 **3.2 Scenario 1: Nominally 'stationary' walking traffic**

367 Eight tests, five focused on the first mode of the structure and three focused on the

368 second mode, were conducted using this loading scenario. The tight-circle walking

369 pattern (Figure 5a) of this scenario is designed in a way that walking people can be

370 assumed 'stationary' on the structure. This approximately eliminates the time-variance

371 of the modal properties of the structure due to change of location of the people walking

372 along the structure and makes possible to use Equation 2 without any further

373 assumptions. As previously mentioned, the centre of the circular walking path is used

374 as the constant location of all walking people.

375 Table 4 presents the test-accepted ranges of human model f_h and ζ_h resulting from this

376 identification process. Figure 9 presents a typical set of occupied structure analytically

377 calculated FRFs (dark grey curves) for test 1.1C (Table 4) when f_h and ζ_h were chosen

378 from their corresponding test-accepted ranges 2.75-3.25Hz and 25-35%, respectively.

379 As it can be seen in this figure, any combination of f_h and ζ_h selected from the

380 corresponding test-accepted ranges (Figure 9 – dark grey FRFs) approximate occupied

381 structure dynamics (Figure 9 – dashed blue FRF) quite well.

382

Table 4: Test-accepted ranges of SDOF human model parameters – Scenario 1

| Test No.	No. of Pedestrians	Location	Average human mass (kg)	Acceptable ranges of SDOF human model parameters				
				f_h (Hz)		m_h (kg)	ζ_h (%)	
				Min	Max		Min	Max
Mode 1 (Structure)								
1.1C	3	Mid-span	70	2.75	3.25	70	25.0	35.0
1.2C	6	Mid-span	70	2.75	3.25	70	25.0	32.5
1.3C	10	Mid-span	70	2.25	3.00	70	25.0	30.0
1.4C	6	3/8 -span	70	2.50	3.20	70	27.5	35.0
1.5C	6	Quarter-span	70	2.50	3.40	70	27.5	40.0
Mode 2 (Structure)								
2.1C	3	Quarter-span	70	5.75	7.75	70	10.0	20.0
2.2C	6	Quarter-span	70	5.50	6.75	70	12.5	20.0
2.3C	10	Quarter-span	70	5.75	6.75	70	12.5	17.5

383
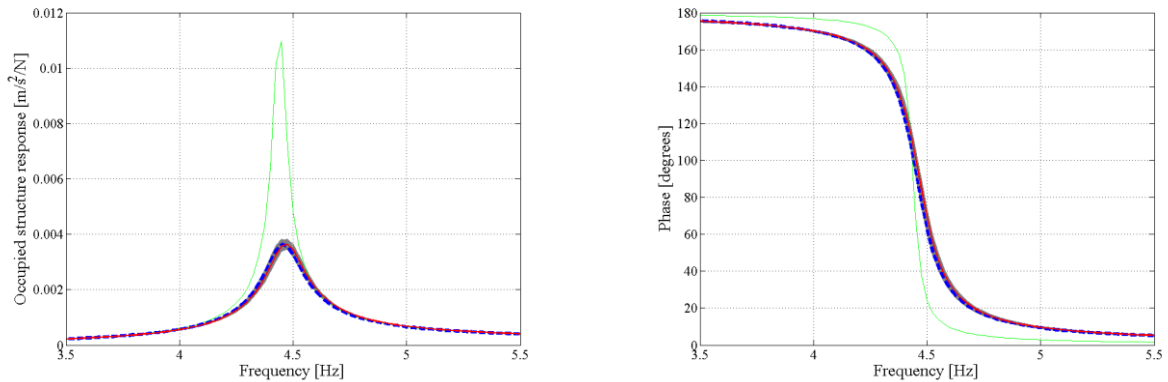
Figure 9:A typical over plot of occupied structure FRF graphs resulted from accepted human model parameters (Grey curves) – Test No 1.1C – (3 pedestrians walking at mid-span – Empty structure: green; Experimental: dashed blue; Best analytical match: red)

384

3.3   Scenario 2: Moving along the structure

386   Scenario 2 comprised 15 tests in which pedestrians were walking along the structure

387   freely and therefore their locations on the structure changed with time. As locations of

388   people in this scenario could not be assumed stationary, Equation 2 could not be used

389   directly. To address this problem, two methods (Method 1 and Method 2) were

390   developed to approximate moving people with a series of stationary cases. Using these

391   methods made it possible to use the Equation 2 to find the occupied structure modal

392   properties under the moving pedestrians load.

393   3.3.1   Method 1

394   Method 1 was based on the assumption that a moving traffic with constant flow of

395   pedestrians can be simulated using a series of pre-defined location patterns and their

396   corresponding probability of occurrence. For each test, a series of pre-defined location

397   patterns similar to the one presented in Figure 10 was defined. These patterns were

398   defined in a way that if pedestrians go through them repeatedly, they create a traffic

399   flow similar to the actual traffic of the corresponding test. The structure and its two side

400 platforms (shown in Figure 1) were divided into 9 segments of equal size. Assuming

401 that all pedestrians were walking with an equal constant speed, the probabilities of

402 pedestrian occurrence in each of the nine segments were equal i.e. 1/9.
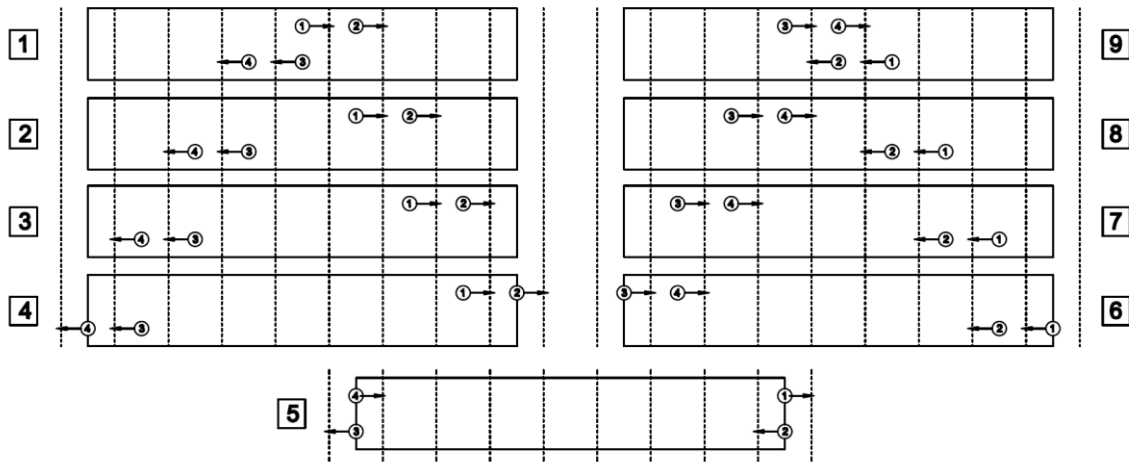

Figure 10: The illustration of pre-defined location patterns for the group of 4 pedestrians

403 Figure 10 shows a typical example of location patterns for a group of four people

404 walking on the test footbridge. Nine location patterns with equal probability of

405 occurrence were defined for this walking group, among which, the pairs of patterns 1

406 and 9, 2 and 8, 3 and 7, and 4 and 6 create the same dynamic effect on the structure.

407 This is because the mode 1 shape is symmetric and the mode 2 shape is anti-symmetric

408 with respect to the mid-span point. Therefore, 5 unique location patterns with the

409 following probabilities were considered for this test:

410 • Pattern 1 (or 9) - Probability: 2/9

411 • Pattern 2 (or 8) - Probability: 2/9

412 • Pattern 3 (or 7) - Probability: 2/9

413 • Pattern 4 (or 6) - Probability: 2/9

414 • Pattern 5: - Probability: 1/9

415   For each location pattern, pedestrians were assumed stationary and Equation 2 was used

416   to simulate the stationary traffic-structure system. The resulting occupied structure

417   modal properties f_{os} and ζ_{os} (and resulting FRF), were then averaged for all location

418   patterns based on their probability of occurrence. The resulting average FRF found for

419   the structure in each simulation was assumed to represent the occupied structure FRF.

420   These FRFs were later compared with their experimental counterpart to find the test-

421   accepted ranges of human model f_h and ζ_h.

422   Figure 11 shows a typical over plot of the occupied structure FRFs for five pre-defined

423   location patterns (grey curves) and the average FRF (red) corresponding to test 1.2

424   (Table 5). The good match between the average analytical and experimental FRF curves

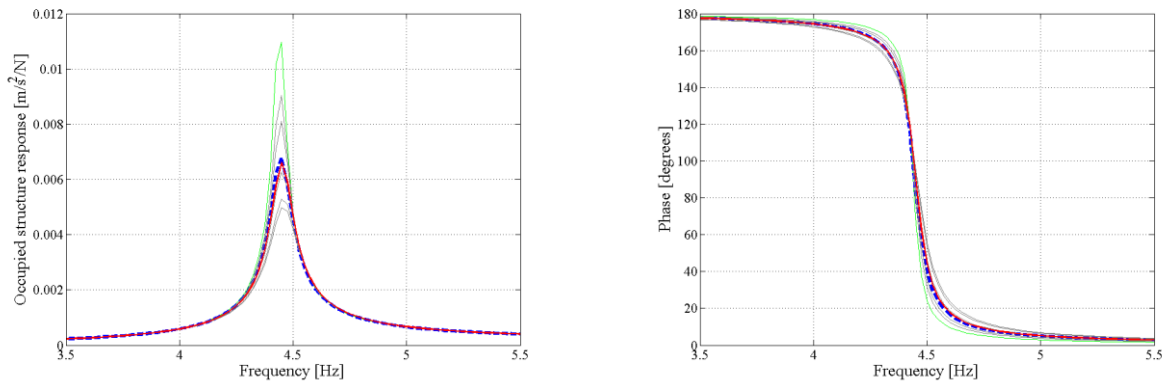425   (dashed blue) can be seen in this figure.

Figure 11: A typical over plot of occupied structure FRF graphs for different location patterns and the average FRF– Test 1.2 – (Empty structure: Green; Curves corresponding to different patterns: grey; Average analytical: red; Experimental: dashed blue)

426   The test-accepted ranges of human model f_h and ζ_h resulting from simulations are

427   presented in Table 5. The over-plot of average occupied structure FRFs for test-accepted

428   f_h and ζ_h ($2.5\text{Hz} < f_h < 3.0\text{Hz}$ and $25\% < \zeta_h < 40\%$) corresponding to test 1.2 is presented

429   in Figure 12. As it can be seen, similar to Scenario 1, any combination of f_h and ζ_h

430   selected from the corresponding test-accepted ranges (dark grey FRFs – 77

431   combinations, i.e. FRFs, in total) approximate the occupied structure dynamics (dashed

432   blue FRF) quite well.

Table 5: Test-accepted ranges of SDOF human model parameters – Scenario 2- Method 1

| Test No.	No. of Pedestrians	Location	Average human mass (kg)	f_h (Hz)		m_h (kg)	ζ_h (%)	
				Min	Max		Min	Max
Mode 1 (Structure)								
1.1	2	All-over	55	2.50	3.50	55	22.5	40.0
1.2	3	All-over	70	2.50	3.00	70	25.0	40.0
1.3	4	All-over	55	2.25	3.50	55	22.5	37.5
1.4	6	All-over	55	2.50	3.25	55	20.0	30.0
1.5	6	All-over	70	2.50	3.25	70	22.5	32.5
1.6	10	All-over	70	2.50	3.25	70	27.5	32.5
1.7	10	All-over	60	2.75	3.25	60	22.5	32.5
1.8	15	All-over	70	2.50	3.00	70	27.5	32.5
Mode 2 (Structure)								
2.1	3	All-over	80	6.50	8.00	80	10.0	20.0
2.2	6	All-over	55	6.50	7.25	55	10.0	17.5
2.3	6	All-over	70	5.75	7.00	70	10.0	20.0
2.4	8	All-over	75	5.50	6.75	75	10.0	17.5
2.5	10	All-over	55	6.00	7.00	55	10.0	17.5
2.6	10	All-over	70	5.75	6.75	70	10.0	20.0
2.7	15	All-over	70	5.00	6.75	70	10.0	17.5

433
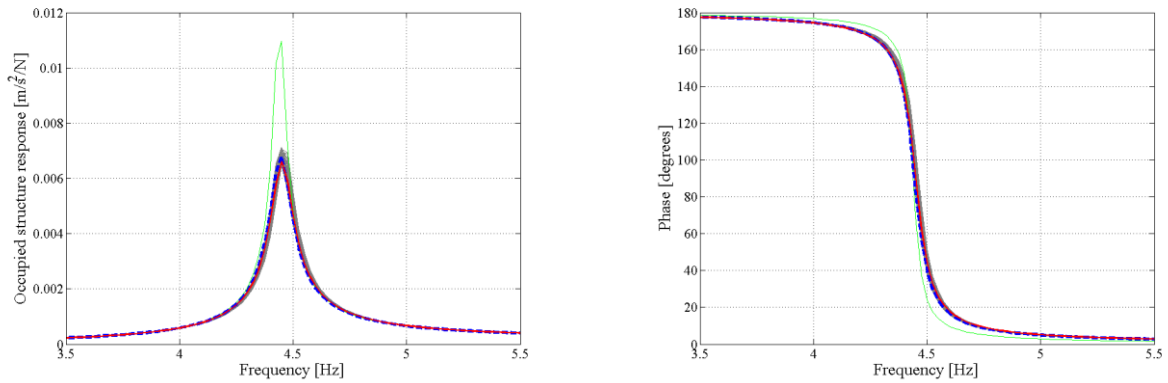
Figure 12: A typical over plot of average occupied structure FRF graphs resulted from accepted human model parameters (Grey curves) – Test 1.2– (Empty structure: green; Average analytical: red; Experimental: dashed blue)

434   3.3.2   Method 2

435   The second method takes the procedure of location simulation one step forward and

436   uses the instantaneous location of each person recorded during each test. For each time-

437   step, location of each pedestrian on the structure was read from the corresponding

438   recorded location time-histories (Figure 4). The walking people were assumed

439   stationary at their locations for that time-step and stationary traffic-structure model

440   (Equation 2) was used to find the occupied structure modal properties for that particular

441   time-step. This kind of simulation was repeated for all time-steps of each test. Using

442   this procedure, time-histories of the change of the occupied structure modal parameters

443     $f_{os}(t)$, $\zeta_{os}(t)$ and $m_{os}(t)$ for each test were found. A typical time-history of $f_{os}(t)$ and $\zeta_{os}(t)$

444   resulting from a random pair of test-accepted f_h and ζ_h corresponding to test 1.2 is
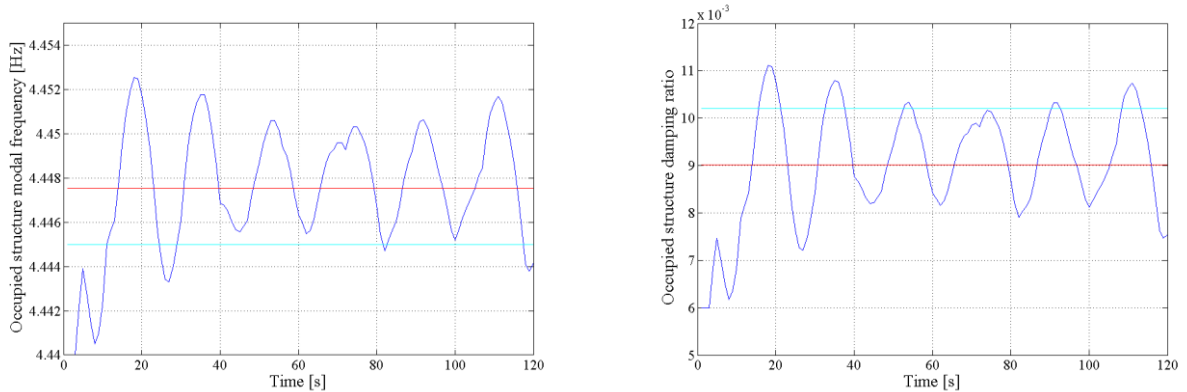
445   presented in Figure 13.

Figure 13: A typical time-history of f_{os} and ζ_{os} (blue), average value(red) and experimental value (cyan) resulted from a typical accepted human model parameter set – Test No 1.2 – (3 pedestrians)

446   The $f_{os}(t)$ and $\zeta_{os}(t)$ were then averaged for each test over time and the averaged

447   parameters (and the corresponding FRF) were assumed to represent the dynamics of the

448   occupied structure. These FRFs were later compared to their experimental counterpart

449   to find the test-accepted ranges of human model f_h and ζ_h.

450   The test-accepted ranges of SDOF human model parameters f_h and ζ_h found in these

451   simulations are presented in Table 6. The over plotted occupied structure FRFs

452   corresponding to the test-accepted f_h and ζ_h (in test 1.2) are presented in Figure 14. As

453   it can be seen, similar to the results of Method 1, any combination of f_h and ζ_h selected

25

454   from the corresponding test-accepted ranges approximated the occupied structure

455   dynamics quite accurately.

Table 6: Test-accepted ranges of SDOF human model parameters – Scenario 2: Method 2

Test No.	No. of Pedestrians	Location	Average human mass (kg)	f_h (Hz) Min	f_h (Hz) Max	m_h (kg)	ζ_h(%) Min	ζ_h(%) Max
Mode 1 (Structure)								
1.1	2	All-over	55	2.50	3.50	55	20.0	40.0
1.2	3	All-over	70	2.25	3.25	70	20.0	40.0
1.3	4	All-over	55	2.25	3.25	55	25.0	37.5
1.4	6	All-over	55	2.50	3.25	55	20.0	30.0
1.5	6	All-over	70	2.25	3.00	70	22.5	32.5
1.6	10	All-over	70	2.50	3.00	70	25.0	32.5
1.7	10	All-over	60	2.75	3.00	60	22.5	30.0
1.8	15	All-over	70	2.25	3.00	70	27.5	32.5
Mode 2 (Structure)								
2.1	3	All-over	80	6.50	7.75	80	10.0	17.5
2.2	6	All-over	55	6.50	7.50	55	10.0	17.5
2.3	6	All-over	70	6.00	6.75	70	10.0	20.0
2.5*	10	All-over	55	6.00	7.00	55	10.0	17.5
2.6	10	All-over	70	6.00	6.75	70	10.0	17.5

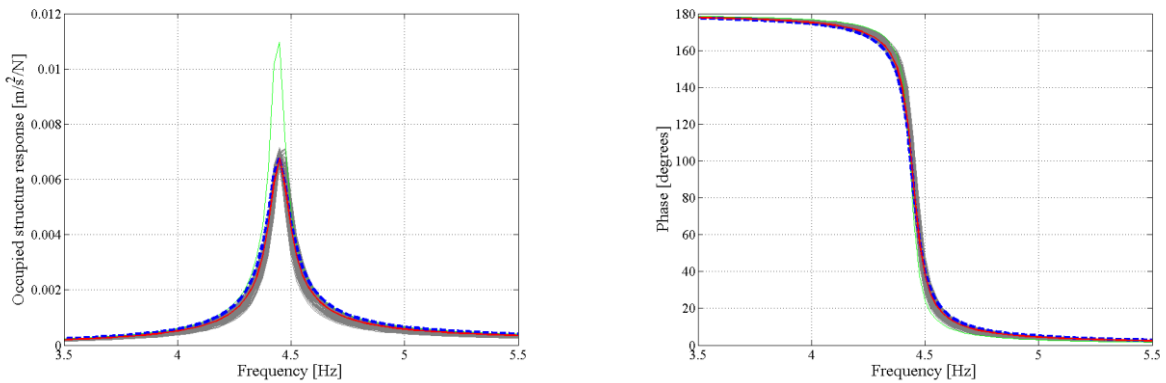* 2.4 and 2.7 are not analyzed as location time history was not available.

456

Figure 14: A typical over plot of empty (green), test-accepted occupied structure FRF graphs (grey), analytical average FRF (red) and experimental FRF (blue) resulted from test-accepted human model parameters – Test 1.2 – (3 pedestrians)

457

458

459   **3.4**   **Common ranges of human model parameters**

460   The test-accepted ranges found in all simulations of both scenarios were compared and

461   a common range was found for f_h and ζ_h for each of the two modes. For the tests targeting

462   the first mode of the test structure, these common ranges (between the pink and green

463   lines, as shown in Figure 15) were found to be 2.75 – 3.00 Hz for f_h and 27.5 % – 30%

464   for ζ_h. These ranges were found to be 6.5 – 6.75 Hz and 12.5 % – 17.5% respectively

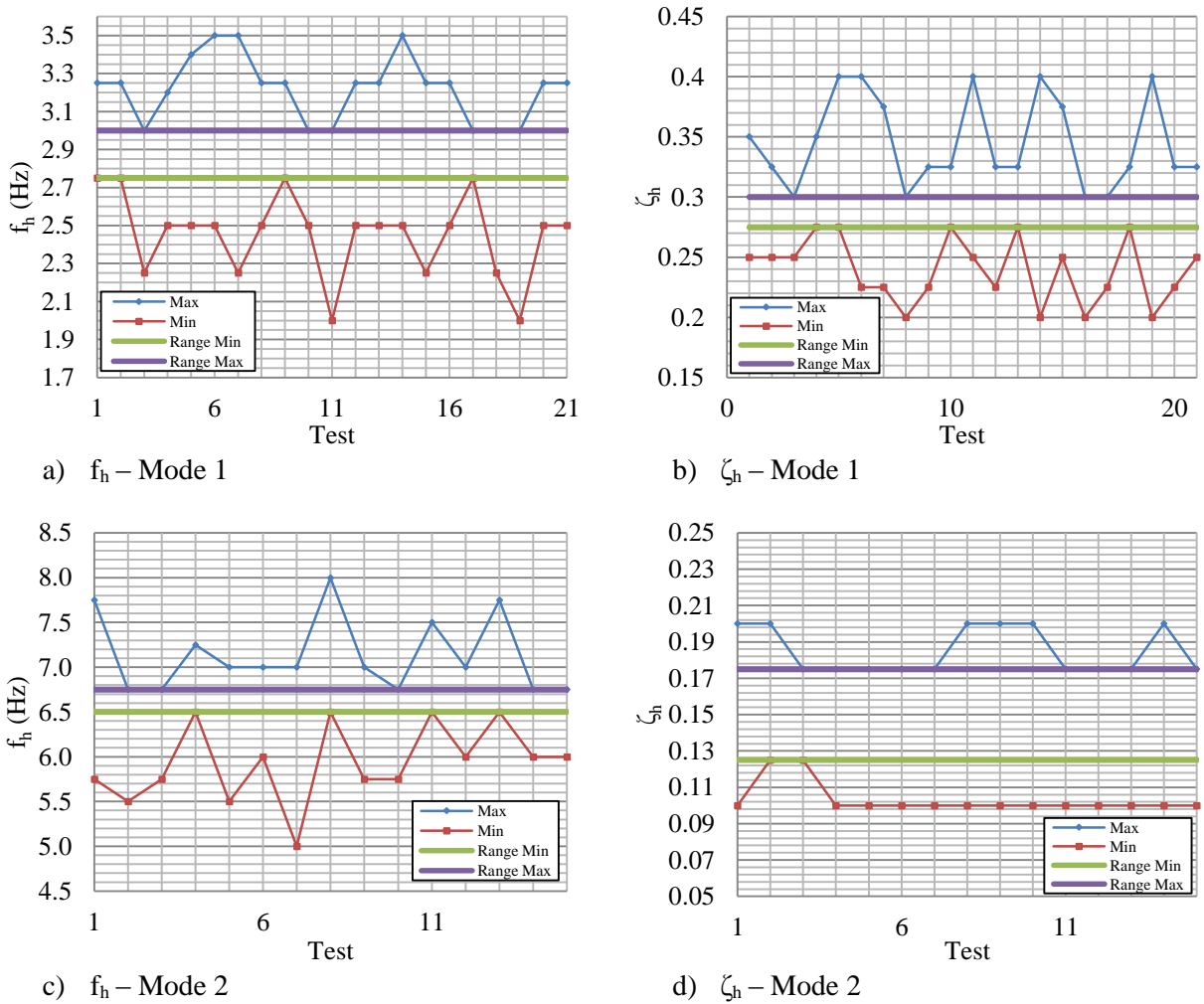465   for the tests targeting the second mode of the structure.

a) f_h – Mode 1   b) ζ_h – Mode 1

c) f_h – Mode 2   d) ζ_h – Mode 2

Figure 15: Test-accepted ranges of f_h and ζ_h found in different tests and their common ranges

466

467

3.5 Expected errors

To understand how good each arbitrary combination of f_h and ζ_h selected from their common ranges (across all tests) can predict the occupied structure dynamics, simulations were repeated for all mode 1 tests but this time with common ranges of f_h and ζ_h as input. The occupied structure parameters f_{os}, ζ_{os} and a_{FRF} were estimated for each combination of f_h and ζ_h and compared with their corresponding experimental values to find the associated errors. The absolute errors associated with the estimated f_{os}, ζ_{os} and a_{FRF} for each combination of f_h and ζ_h were averaged over all tests and presented in Figure 16. As it can be seen in these graphs, the minimum errors of estimating f_{os}, ζ_{os} and a_{FRF} were not associated with a unique set of f_h and ζ_h i.e. no particular set of f_h and ζ_h can predict all f_{os}, ζ_{os} and a_{FRF} with minimum error at the same time. However, for engineering purposes, it is clear that errors are so small that any combination of the f_h and ζ_h from the identified common ranges would yield good approximation of the occupied structure modal properties for any number of up to 15 pedestrians.
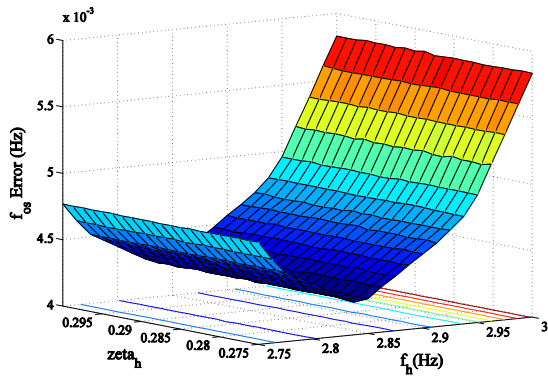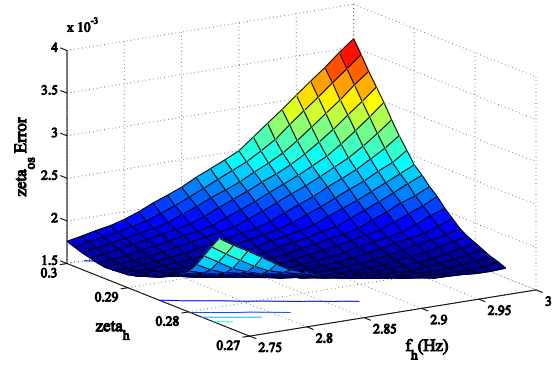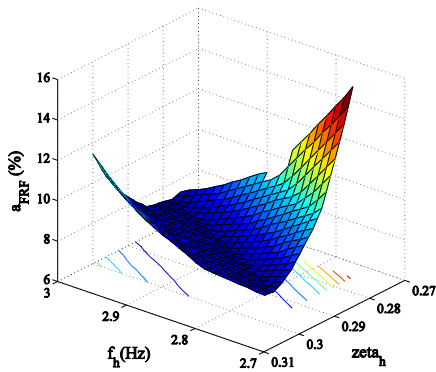
a) f_{os} Error

b) ζ_{os} Error

c) a_{FRF} Error

Figure 16: Expected errors in occupied structure natural frequency f_{os}, damping ratio ζ_{os} and peak FRF magnitude a_{FRF} for the common ranges of human model parameters –Mode 1

487

4 Comparison with other published findings

488

489 The works of Silva and Pimentel [41] and Jiménez-Alonso and Sáez [44] are the only

490 examples to date known to the authors that specifically investigated parameters for the

491 SDOF walking human model in the context of structural vibration serviceability. Silva

492 and Pimentel [41] identified the parameters of an SDOF MSD walking human model

493 by analyzing the correlation of the walking force and the acceleration of the human body

494 recorded at waist. Assuming human mass equal to 70kg and 1.8Hz mean pacing

495 frequency, their model suggests f_h=2.64Hz and ζ_h = 0.55 for an SDOF walking human

496 model.

29

497   Jiménez-Alonso and Sáez [44] used a 3DoFs model, comprised of three independent

498   SDOF MSD to simulate interaction of a walking human with a structure in each

499   direction. They used the experimental data reported by Georgakis and Jorgesen [57] in

500   an inverse dynamics procedure to identify the parameters of the SDOF human model in

501   the vertical direction by trial and error. Their study suggested that an SDOF MSD model

502   with a mass equal to 84% of the total body mass, damping ratio of 47% and natural

503   frequency of 2.75Hz can simulate dynamic effects of a walking human on structures in

504   the vertical direction.

505   The walking human model parameters suggested by both studies are comparable with

506   the findings of this research for the first vertical mode of structure although the damping

507   ratios proposed are slightly higher than what is presented in this paper..

508   Findings of this research are also in line with the findings of Shahabpoor et al. [34].

509   Based on an analytical study of 2DOF MSD model of a crowd-structure system, they

510   suggested that when the natural frequency of the occupied structure f_{os} is higher than

511   that of the empty structure fes, the natural frequency of the human/crowd model f_h is

512   lower than the natural frequency of the empty structure $f_h < f_{es}$.

5   Conclusions

514   The work presented in this paper used a comprehensive and unique set of human traffic-

515   structure experimental data to identify the parameters of the SDOF walking human

516   model. Three different identification processes were applied with increasing level of

517   detail for simulating the effects of location of each individual as they walk on the

518   structure. The analysis of effects of HSI on the fundamental vertical mode of the

519   structure yielded the ranges of $2.75 - 3.00$Hz and $27.5\% - 30\%$ for the natural frequency

520   and damping ratio of the SDOF MSD walking human model, respectively. These ranges

521   were found to be $6.5 - 6.75$ Hz and $12.5 \% - 17.5\%$ respectively for the tests targeting

522   the second vertical mode of the structure, indicating likely presence of the higher mode

523   of the human body which got engaged more within the frequency range of the second

524   mode of the structure. The measured average mass of people of 70 kg was used as the

525   SDOF mass of the walking human model. The different *walking* human model

526   parameters found for the first two vertical vibration modes of the structure is the key

527   novel finding and can be an indicator of MDOF nature of walking human model.

528   These results compare reasonably well with independently proposed values reported in

529   the only directly relevant works to date done by Silva, et al. [41] and Jiménez-Alonso

530   and Sáez [44]. The comprehensive experimental data, variety of loading scenarios,

531   detailed simulation process and coherent results from different methods provide high

532   level of confidence about the validity of the findings.

533   The experimental data set used in this research can serve as a benchmark for data

534   collection for future multi-pedestrian HSI studies. Moreover, the proposed

535   methodologies for simulating time-varying location of the walking people on the

536   structure proved to be accurate and practically applicable, so they can be used by design

537   engineers to simulate the walking traffic.

538   Further research on different real-life structures is needed using the proposed

539   methodology to extend and validate the findings of this research for different structures

540   and loading scenarios.

Acknowledgements

References

[1] Tredgold, T., 1828. Elementary principles of carpentry. 2nd edition.

[2] Figueiredo, F.P., da Silva, J.G.S., de Lima, L.R.O., da S. Vellasco, P.C.G. and de Andrade, S.A.L., 2008. A parametric study of composite footbridges under pedestrian walking loads. Engineering Structures, 30, pp.605–615.

[3] Živanović, S., Pavic, A. and Reynolds, P., 2005. Vibration serviceability of footbridges under human-induced excitation: a literature review. Journal of Sound and Vibration, 279(1–2), pp.1-74. ISSN 0022-460X.

http://dx.doi.org/10.1016/j.jsv.2004.01.019.

[4] Racic, V., Pavic, A., and Brownjohn, J.M.W., 2009. Experimental identification and analytical modelling of human walking forces: Literature review. Journal of Sound and Vibration, 326(1–2), pp.1–49.

[5] Ingólfsson, E.T., Georgakis, C.T., Ricciardelli, F., and Jönsson, J., 2012. Experimental identification of pedestrian-induced lateral forces on footbridges. Journal of Sound and Vibration, 330(6), pp.1265–1284.

[6] Caprani, C.C., 2014. Application of the pseudo-excitation method to assessment of walking variability on footbridge vibration. Computers and Structures, 132, pp. 43–54.

[7] Pimentel, R.L., Pavic, A., and Waldron, P. 2001. Evaluation of design requirements for footbridges excited by vertical forces from walking. Canadian Journal of Civil Engineering, 28(5), pp.769–777. doi:10.1139/l01-036.

[8] Živanović, S., Pavic, A. and Ingolfsson, E.T., 2010. Modelling spatially unrestricted pedestrian traffic on footbridges. Journal of Structural Engineering, 136 (10), pp.1296 – 1308.

33

573   [9] Brownjohn, J.M.W., Fok, P., Roche, M. and Omenzetter, P., 2004. Long span steel

574   pedestrian bridge at Singapore Changi Airport—part 2: crowd loading tests and

575   vibration mitigation measures. Structural Engineer, 82 (16), pp.28–34.

576   [10] Kasperski, M., Sahnaci C., 2007. Serviceability of pedestrian structures.

577   Proceedings of the 25th international modal analysis conference, Orlando, Florida.

578   pp.774–98.

579   [11] Shahabpoor, E., Pavić, A., 2012. Comparative evaluation of current pedestrian

580   traffic models on structures. Conference Proceedings of the Society for Experimental

581   Mechanics Series, 26, pp 41-52.

582   [12] The International Federation for Structural Concrete (FIB), 2005. Guidelines for

583   the design of footbridges.

584   [13] International Organization for Standardization (ISO), 2007. Bases for design of

585   structures: Serviceability of buildings and walkways against vibrations. ISO

586   10137:2007, Geneva.

587   [14] Technical Department for Transport, Roads and Bridges Engineering and Road

588   Safety/French Association of Civil Engineering (SETRA/AFGC), 2006. Footbridges:

589   Assessment of vibrational behavior of footbridges under pedestrian loading. Technical

590   Guide 0611, Paris.

591   [15] British Standards Institution (BSI), 2008. UK national annex to Eurocode 1:

592   Actions on structures. Part 2: Traffic loads on bridges, NA to BS EN 1991-2:2003

593   London.

594   [16] Ingólfsson, E.T., Georgakis, C.T., and Svendsen, M.N. 2008. Vertical footbridge

595   vibrations: Details regarding and experimental validation of the response spectrum

596   methodology. Proceeding of Footbridge conference.

597   [17] Brownjohn, J.M.W., Pavic, A. and Omenzetter, P.A., 2004. Spectral density

598   approach for modeling continuous vertical forces on pedestrian structures due to

599   walking. Canadian Journal of Civil Engineering, 31(1), pp.65–77.

600   [18] Racic, V. and Brownjohn, J.M.W., 2011. Stochastic model of near-periodic vertical

601   loads due to humans walking. Advanced Engineering Informatics, 25, pp.259–75.

602   [19] Živanović, S., Pavic, A. and Reynolds, P., 2007. Probability-based prediction of

603   multi-mode vibration response to walking excitation. Engineering Structures, 29(6),

604   pp.942–54.

605   [20] Živanović, S. and Pavic, A., 2009. Probabilistic modelling of walking excitation

606   for building floors. Journal of Performance of Constructed Facilities, 23(3), pp.132 –

607   143.

608   [21] Piccardo, G. and Tubino, F., 2012. Equivalent spectral model and maximum

609   dynamic response for the serviceability analysis of footbridges. Engineering Structures,

610   40(7), pp.445–56.

611   [22] Krenk, S., 2012. Dynamic response to pedestrian loads with statistical frequency

612   distribution. ASCE Journal of Engineering Mechanics, 138(10), pp.1275–81.

613   [23] Griffin, M.J., 1990. Handbook of human vibration, Academic Press, London.

614   [24] Racic, V., Brownjohn, J.M.W., Pavic, A., 2010. Reproduction and application of

615   human bouncing and jumping forces from visual marker data. Journal of Sound and

616   Vibration, 329, pp.3397-3416.

617   [25] Sachse, R., Pavic, A. and Reynolds, P., 2002. The Influence of a Group of Human

618   Occupants on Modal Properties of a Prototype Assembly Structure. Proceeding of the

619   5th European Conference on Dynamics EURODYN, pp.1241-1246.

620   [26] Sachse, R., Pavic, A. and Reynolds, P., 2003. Human-structure dynamic interaction

621   in civil engineering dynamics: A literature review. The Shock and Vibration Digest,

622   35(1), pp.3-18. ISSN 0583-1024.

623   [27] Butz, C., Feldmann, M. and Heinemeyer, C., 2008. Advanced load models for

624   synchronous pedestrian excitation and optimized design guidelines for steel footbridges.

625   RFSRCT- 2003-00019, European Commission, Brussels, Belgium.

626   [28] Reynolds, P., Pavic, A. and Ibrahim, Z., 2004. Changes of Modal properties of a

627   stadium structure occupied by a crowd. Proceeding of the 22nd International Modal

628   Analysis Conference (IMAC XXII).

629   [29] Salyards, K. and Firman, R., 2011. Human-structure interaction effects of crowd

630   characteristics. Conference Proceedings of the Society for Experimental Mechanics

631   Series, Civil Engineering Topics, 4, pp.247-254.

632   [30] Fitzpatrick, A., Dallard, P., le Bourva, S., Low, A., Ridsill Smith, R. and Willford,

633   M., 2001. Linking London: The Millennium Bridge. The Royal Academy of

634   Engineering, London.

635   [31] Bocian, M., Macdonald, J., and Burn, J., 2012. Biomechanically inspired modelling

636   of pedestrian-induced forces on laterally oscillating structures. Journal of Sound and

637   Vibration, 331, pp.3914–3929. http://dx.doi.org/10.1016/j.jsv.2012.03.023

638   [32] Barker, C., and Mackenzie, D., 2008. Calibration of the UK National Annex. The

639   Proceedings of the Third Footbridge International Conference, Porto, Portugal.

640   [33] Živanović, S., Diaz, I.M. and Pavić, A., 2009. Influence of walking and standing

641   crowds on structural dynamic properties. Proceeding of Conference & Exposition on

642   Structural Dynamics (IMAC XXVII).

643   [34] Shahabpoor, E., Pavić, A. & Racic, V., 2013. Using MSD Model to Simulate

644   Human-Structure Interaction during Walking. Conference Proceedings of the Society

645   for Experimental Mechanics Series.

646   [35] Shahabpoor, E., Pavić, A. & Racic, V., 2013. Sensitivity Analysis of Coupled

647   Crowd-structure System dynamics to Walking Crowd Properties. Conference

648   Proceedings of the 5th International Conference on Structural Engineering, Mechanics

649   and Computation (SEMC 2013).

650   [36] Miyamori, Y., Obata, T., Hayashikawa, T., Sato, K., 2001. Study on identification

651   of human walking model based on dynamic response characteristics of pedestrian

652   bridges, in: Proceedings of the Eighth East Asia-Pacific Conference on Structural

653   Engineering & Construction (EASEC-8), Singapore.

654   [37] Kim, S.H., Cho, K.I., Choi, M.S., and Lim, J.Y. 2008. Development of human body

655   model for the dynamic analysis of footbridges under pedestrian induced excitation.

656   International Journal of Steel Structures, 8(4), pp.333–345.

657   [38] International Organization for Standardization (ISO), 1981. Mechanical driving

658   point impedance of the human body. ISO 5982:1981.

659   [39] Archbold, P.j., 2004. Interactive load models for pedestrian footbridges. PhD

660   Thesis, University College Dublin.

661   [40] Archbold, P.J., Keogh, J., Caprani, C., and Fanning. P., 2011. A Parametric Study

662   of Pedestrian Vertical Force Models for Dynamic Analysis of Footbridges. Proceeding

663   of Experimental Vibration Analysis for Civil Engineering Structures Conference

664   (EVACES 2011).

665   [41] Silva, F.T., and Pimentel, R.L., 2011. Biodynamic walking model for vibration

666   serviceability of footbridges in vertical direction. Proceeding of the 8th International

667   Conference on Structural Dynamics (Eurodyn 2011), pp.1090–1096.

668   [42] Silva, F.T. Brito, H.M. and Pimentel. R.L., 2013. Modeling of crowd load in

669   vertical direction using biodynamic model for pedestrians crossing footbridges.

670   Canadian Journal of Civil Engineering, 40, pp.1196–1204.

671   http://dx.doi.org/10.1139/cjce-2011-0587

672   [43] Caprani, C.C., Keogh, J., Archbold, P., and Fanning, P., 2011. Characteristic

673   vertical response of a footbridge due to crowd loading. Proceeding of the 8th

674   International Conference on Structural Dynamics (Eurodyn 2011), pp.978–985.

675   [44] Jiménez Alonso, J.F., Sáez, A., 2014. A direct pedestrian-structure interaction

676   model to characterize the human induced vibrations on slender footbridges. Informes de

677   la Construcción, 66 (EXTRA1):m007, doi: http://dx.doi.org/10.3989/ic.13.110.

678   [45] Qin, J.W., Law, S.S., Yang, Q.S. and Yang, N., 2013. Pedestrian–bridge dynamic

679   interaction, including human participation. Journal of Sound and Vibration, 332(4),

680   pp.1107-1124, ISSN 0022-460X, http://dx.doi.org/10.1016/j.jsv.2012.09.021.

681   [46] Qin, J.W., Law, S.S., Yang, Q.S. and Yang, N., 2014. Finite Element Analysis of

682   Pedestrian-Bridge Dynamic Interaction. Journal of Applied Mechanics, 81(4), DOI:

683   10.1115/1.4024991.

684

685   [47] Bocian, M., Macdonald, J., and Burn, J. 2011. Modelling of self-excited vertical

686   forces on structures due to walking pedestrians. Proceedings of the 8th International

687   Conference on Structural Dynamics (EURODYN 2011) ISBN 978-90-760-1931-4.

688   [48] Bocian, M., Macdonald, J., and Burn, J. 2013. Biomechanically Inspired Modeling

689   of Pedestrian-Induced Vertical Self-Excited Forces. Journal of Bridge Engineering 18,

690   pp.1336–1346.

691   [49] Paulissen, J.H. and Metrikine. A.V., 2011. Non-linear dynamic modelling of

692   adaptive pedestrian behavior on lively footbridges. Proceedings of the 8th International

693   Conference on Structural Dynamics (EURODYN 2011).

694   [50] Pecol, P., Dal Pont, S., Silvano, E., Joanna, B. and Argoul, P., 2011. A 2D discrete

695   model for crowd-structure interaction. Proceeding of the 4th Footbridges international

696   conference.

697   [51] APS Dynamics, 2014. APS 400 ELECTRO-SEIS Long Stroke Shaker with Linear

698   Ball Bearings. Available at:

699   http://www.apsdynamics.com/images/stories/Prospekte/APS_Shaker/APS_400/APS_4

700   00_Data_Sheet_en.pdf [Accessed 10 June 2015].

701   [52] SICK Sensor Intelligence, 2009. LD-PeCo People Counter: Operating instructions.

702   Available at: https://www.sick.com/media/pdf/7/47/247/IM0011247.PDF. Last

703   accessed: 10 June 2015.

704   [53] Clough, W. and Penzien, J., 1993. Dynamics of structures. 2nd edition, McGraw-

705   Hill, New York. ISBN 0-07-011394-7.

706   [54] Frazer, R.A., Duncan, W.J. and Collar, A.R., 1957. Elementary Matrices.

707   Cambridge University Press.

708   [55] Sachse, R., Pavic, A. and Reynolds, P., 2004. Parametric study of modal properties

709   of damped two-degree-of-freedom crowd–structure dynamic systems. Journal of Sound

710   and Vibration, 274, pp. 461–480.

711   [56] Ferris, D. P., Louie, M. and Farley, C. T., 1998. Running in the real world: adjusting

712   leg stiffness for different surfaces. Proceeding of the Royal Society, London, 265, pp.

713   989-994.

714   [57] Georgakis, C.T. and Jorgensen, N.G., 2013. Change in mass and damping on

715   vertically vibrating footbridges due to pedestrians. Proceedings of the 31st Conference

716   on Structural Dynamics (IMAC 2013) 3(4), pp.37-45.